Fig. S1. Human TLS fibroblasts expansion correlates with CD45+ infiltration.
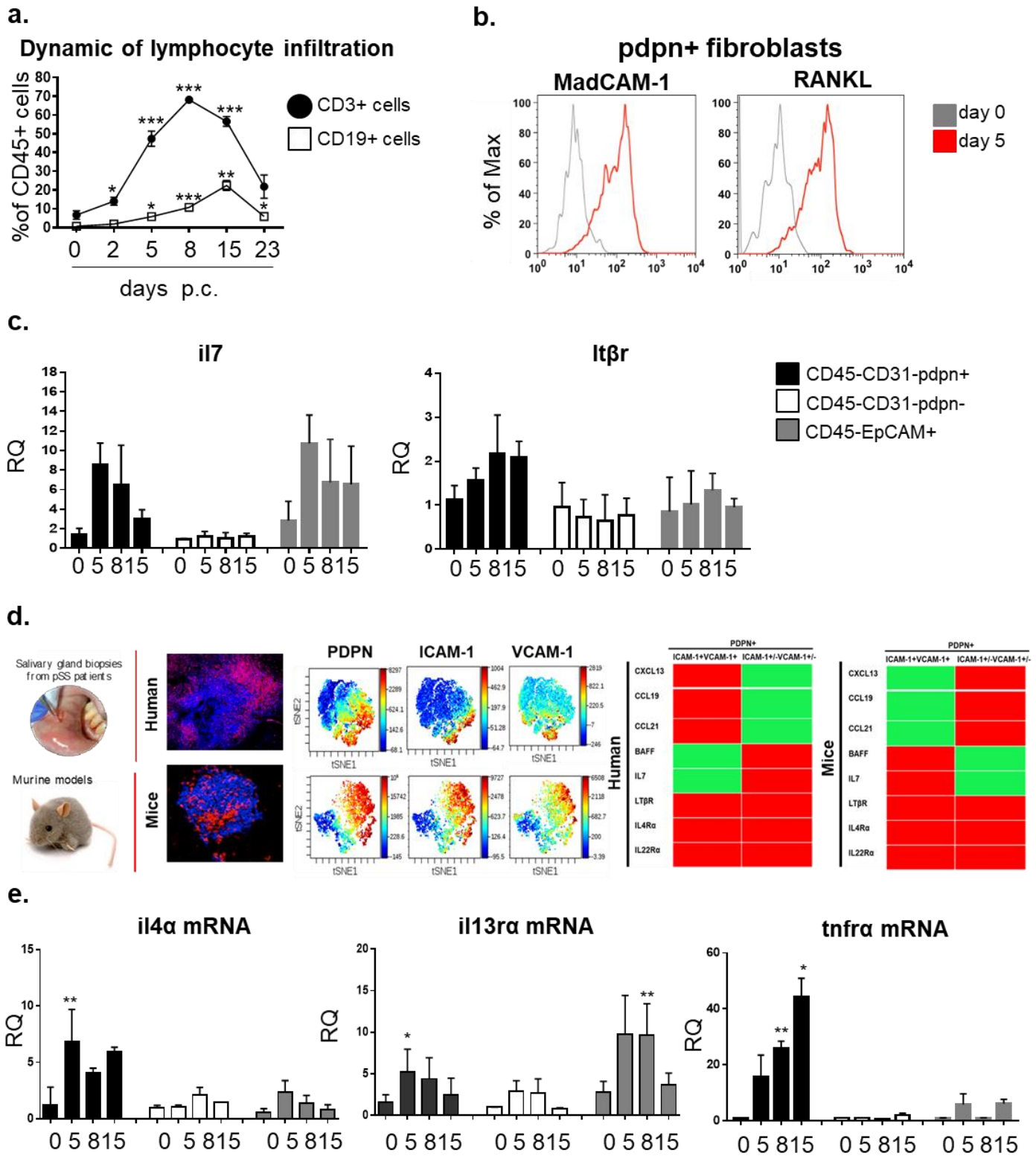
Fig. S2. Inflammation of murine salivary glands results in lymphocytic infiltration and activation of pdpn+ fibroblasts to express lymphoid cytokines and its receptors.
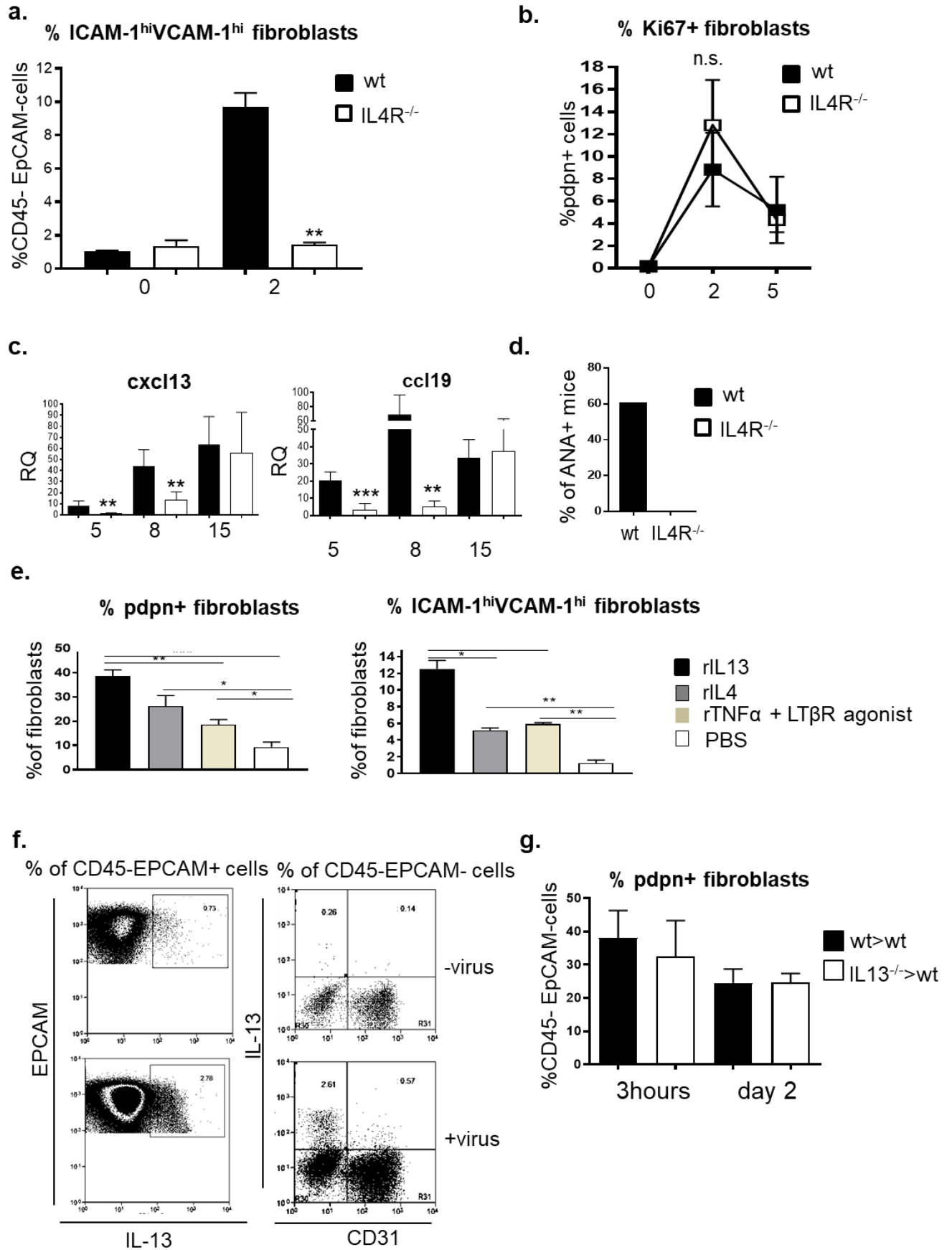
Fig. S3. IL4R engagement via IL13 is crucial for induction of immuno-fibroblasts.
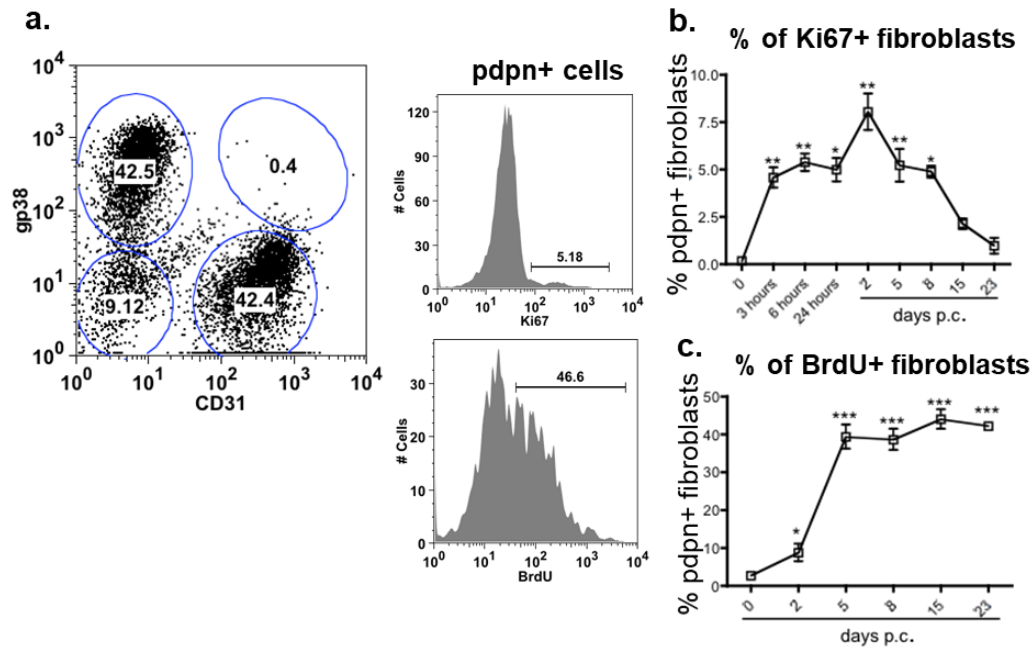
Fig. S4. Proliferative profile of pdpn+ immuno-fibroblasts during salivary gland inflammation.

a.

ICAM-1^{hi}VCAM-1^{hi}

ICAM-1^{int}VCAM-1^{int}

b.

% of proliferating pdpn+ fibroblasts

% of proliferating pdpn+ fibroblasts
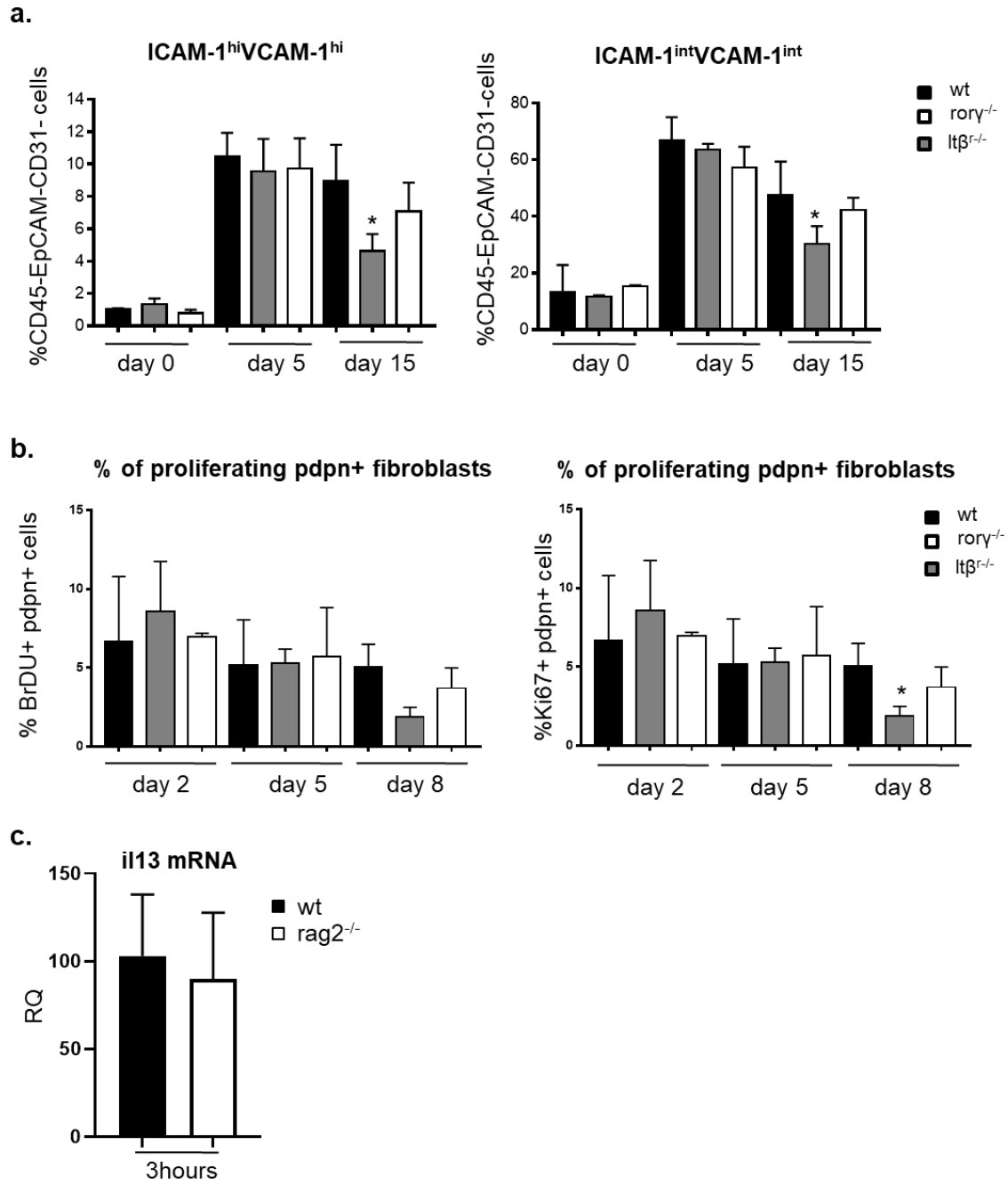
c.

il13 mRNA

Fig. S5. Maintenance but not induction of immuno-fibroblasts during TLS formation is dependent on LTβR.
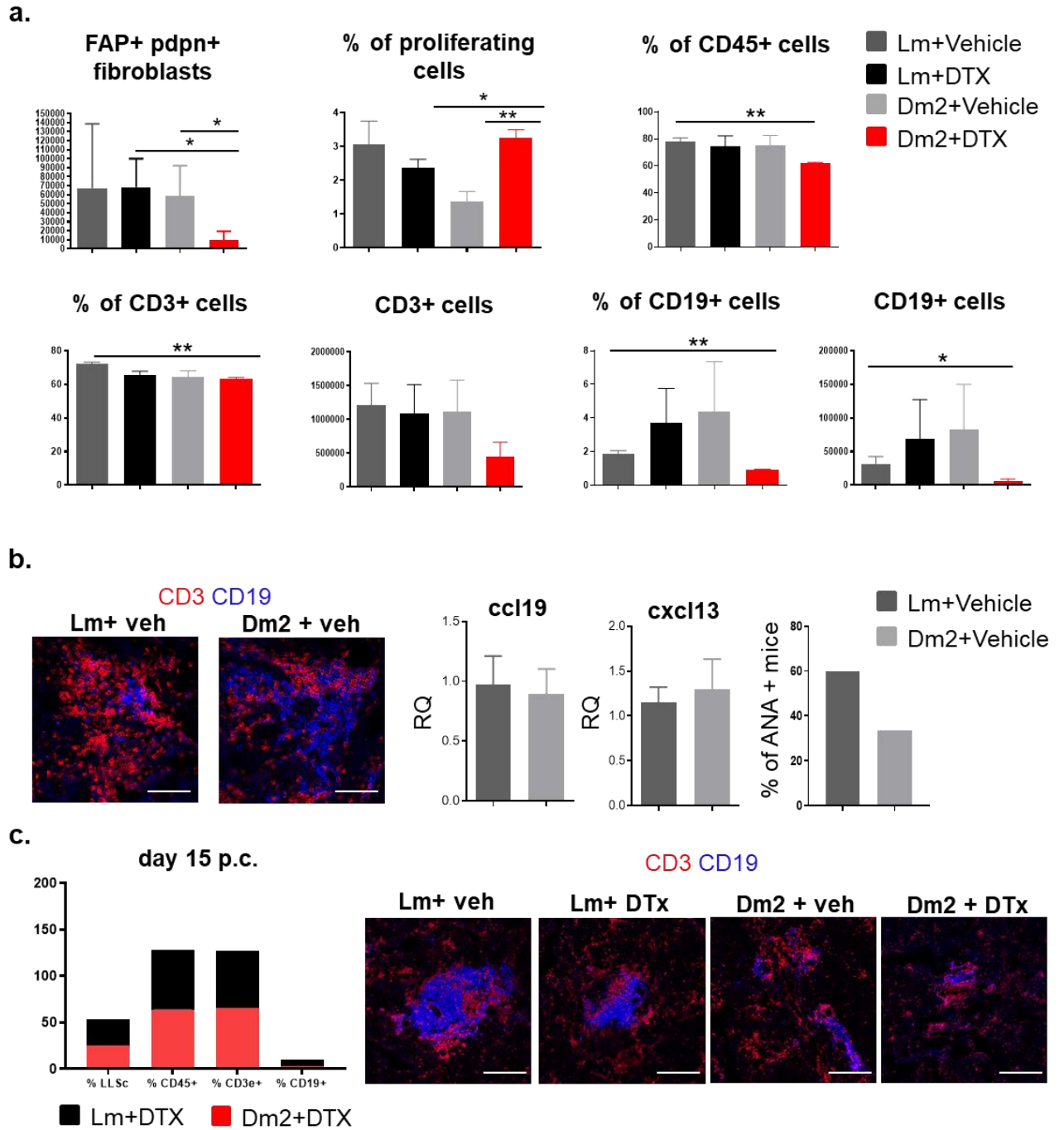
Fig. S6. Pdpn+ FAP+ fibroblasts are fundamental for TLS assembly and maintenance.
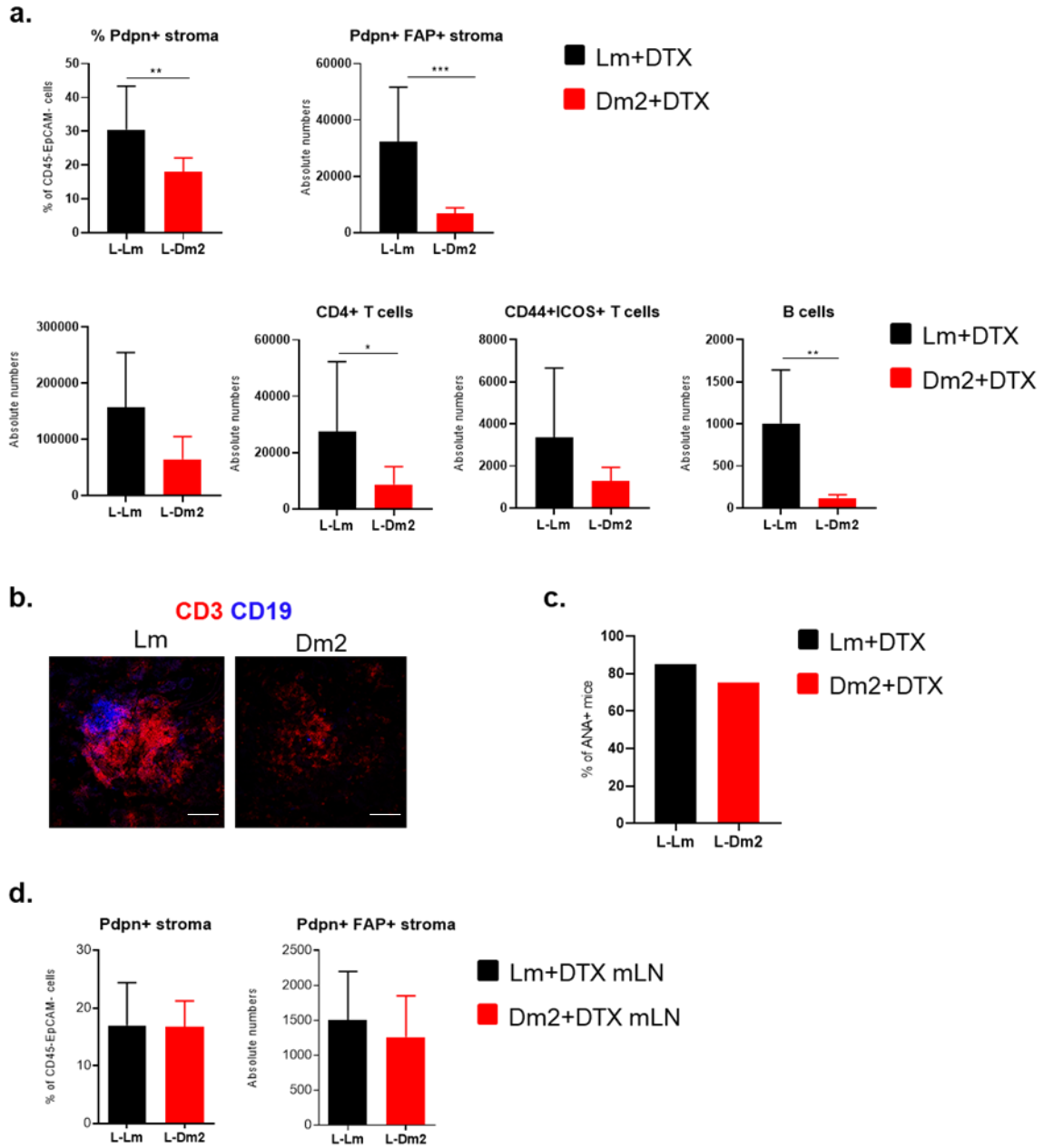
Fig. S7. Local depletion of pdpn+ FAP+ fibroblasts confirms their indispensability for TLS assembly and maintenance.

DTX treatment systemic regimen

DTx 25ng/g

Days -7 -5 0 8 15 23

Salivary gland cannulation
with AdV

Experiment endpoints
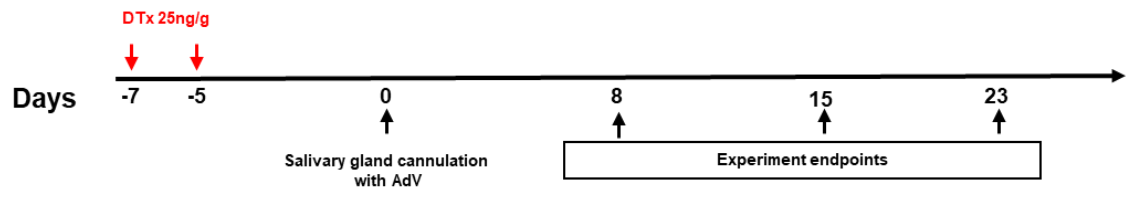
DTX treatment local regimen

DTx 100ng/gland

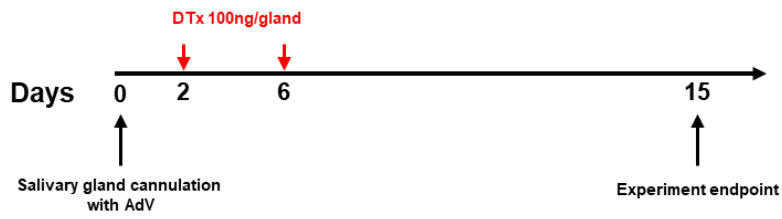Days 0 2 6 15

Salivary gland cannulation
with AdV

Experiment endpoint

Fig. S8. Systemic and local treatment regimens for depletion of pdpn+ FAP+ cells

Fig. S1. Human TLS fibroblasts expansion correlates with CD45+ infiltration.

a. Immunofluorescence analysis of salivary gland biopsy from pSS patient stained for pdpn (red), FAP (green) and DAPI (blue). Scale bar: 250μm. **b.** Linear regression analysis confirms significant (***p<0.001; R square=0.9718) correlation between the percentage of CD45+ cells and percentage of pdpn+ cells in salivary gland biopsies of pSS patients analysed by flow cytometry. **c.** Graph showing expression (median fluorescence intensity) of ICAM-1 and VCAM-1 in CD34+ and CD34- fibroblasts. Represented as mean ± SD, **p<0.01; ***p<0.001; one-way ANOVA. **d.** Gene expression analysis for ltβr and tnfr transcripts on sorted CD34+ and CD34- pdpn+ populations. Data expressed as mean ± SD (*n*=5) Data expressed as mean ± SD (*n*=5), analysed by paired t test for statistical significance. **e.** Representative histogram showing IL22Rα expression by human pdpn+ fibroblasts from pSS salivary gland biopsy. **f.** Expression of *vcam1*, *icam1* and *pdpn* mRNA transcript levels in pSS fibroblasts stimulated *in vitro* with IL22, TNF and LTα1β2 (*n*=5). Data represented as mean ± SD, **p<0.01; ***p<0.001; one-way ANOVA.

Fig. S2. Inflammation of murine salivary glands results in lymphocytic infiltration and activation of pdpn+ fibroblasts to express lymphoid cytokines and its receptors.

a. Time course flow cytometry analysis of percentages of CD3+ and CD19+ cells within the CD45+ compartment. Data expressed as mean ± SD of two independent experiments with 6 biological replicates. *p<0.05; **p<0.01; ***p<0.001, one-way ANOVA. **b.** Expression levels of MadCAM-1 and RANK-L by pdpn+ fibroblasts at days 0 and 5 p.c. **c.** qRT-PCR analysis of il7 and ltbr mRNA transcripts in sorted populations (pdpn+ fibroblasts, pdpn- fibroblasts and EpCAM+ cells) at days 0, 5, 8 and 15 p.c. (*n*=2-8). Represented as mean ± SD. **d.** Diagram highlighting the heterogeneity within pdpn+ fibroblasts in expression of ICAM-1, VCAM-1, lymphoid

chemokines, survival factors, Th2 and IL22Rα in human and mouse pdpn+ cells isolated from inflamed salivary glands. Red represents high expression of the indicated gene and green represent low or no expression of the indicated gene. **e.** qRT-PCR analysis of il4ra, il13ra and tnfra mRNA transcripts in sorted populations (pdpn+ fibroblasts, pdpn- fibroblasts and EpCAM+ cells) at days 0, 5, 8 and 15 p.c. (*n*=2-8). *p<0.05; **p<0.01; one-way ANOVA. Represented as mean ± SD.

Fig. S3. IL4R engagement via IL13 is crucial for induction of immuno-fibroblasts.

a. Proportion of pdpn+ fibroblasts and ICAM-1^{high}VCAM-1^{high} fibroblasts at days 0 and 2 p.c. in wt (black squares, *n*=3-6) and IL4R$^{-/-}$ (open squares, *n*=3-6) **p<0.01; t test. Represented as mean ± SD. **b.** Analysis of proliferating pdpn+ fibroblasts at days 0, 2 and 5 p.c. in wt (black squares, *n*=3-4) and IL4R$^{-/-}$ (open squares, *n*=3-4) by Ki67 flow cytometry staining. Represented as mean ± SD, one-way ANOVA. **c.** Analysis of cxcl13 and ccl19 mRNA from salivary glands at days 5, 8 and 15 p.c. in IL4R$^{-/-}$ mice (white bars, *n*=4-5) in comparison to wt (black bars, *n*=4-5). **p<0.01; ***p<0.001; one-way ANOVA. Represented as mean ± SD. **d.** Percentage of positive mice for ANA in IL4R$^{-/-}$ mice as compared to wt. **e.** Proportion of pdpn+ fibroblasts and ICAM-1^{high}VCAM-1^{high} fibroblasts analyzed by flow cytometry post cannulation with rIL13 (*n*=3), rIL4 (*n*=3), rTNFα and LTβR agonist (*n*=4), and PBS (*n*=4). *p<0.05; **p<0.01; one-way ANOVA. Represented as mean ± SD. **f.** Flow cytometry plots of IL-13 intracellular expression in epithelial cells (CD45-EpCAM+) and fibroblasts (CD45-EpCAM-CD31- cells) at 3 hours with and without virus stimulation. **g.** Graph showing expansion of pdpn+ fibroblasts at 3 hours and day 2 p.c. in wt (black bars, *n*=4) and il13$^{-/-}$ GFP bone-marrow chimera (white bars, *n*=4) salivary glands. Represented as mean ± SD.

Fig. S4. Proliferation status of pdpn+ immuno-fibroblasts at different time-points post-cannulation.

a. FACS histogram representing Ki67+ and BrDU+ pdpn+ fibroblasts in wt mice salivary glands at day 5 p.c. **b-c.** Graphs showing proliferation, both Ki67 and BrdU of CD31-pdpn+ cells in the CD45-EPCAM- cell population. *p<0.05; ** p < 0.01, *** p < 0.001 versus day 0 wt mice; one way ANOVA. Represented as mean ± SD. Data are from three independent experiments with 4 analysed per group.

Fig. S5. Maintenance but not induction of immuno-fibroblasts during TLS formation is dependent on LTβR.

a. Analysis of the percentage of ICAM-1^{high}VCAM-1^{high} fibroblasts and ICAM-1^{int}VCAM-1^{int} fibroblasts in wt (black bars, n=3-5), Rorγ$^{-/-}$ (open bars, n=3-5) and Ltβr$^{-/-}$ (grey bars, n=3-5) mice at days 0, 5 and 15 p.c. *p<0.05, one-way ANOVA. Represented as mean ± SD. **b.** Flow cytometry analysis of BrdU incorporating and Ki67+ pdpn+ fibroblasts at days 2, 5 and 8 p.c. in wt (black bars, n=4-5), Rorγ$^{-/-}$ (open bars, n=3-4) and Ltβr$^{-/-}$ (grey bars, n=3-4) mice. *p<0.05, one-way ANOVA. Represented as mean ± SD. **c.** Analysis of il-13 mRNA from salivary glands at 3hours p.c. in Rag2$^{-/-}$ mice (open bars, n=4) in comparison to wt (black bars, n=4). Represented as mean ± SD.

Fig. S6. Pdpn+ FAP+ fibroblasts are fundamental for TLS assembly and maintenance.

a. Graphs summarizing the FACS data for absolute numbers of FAP+ pdpn+ fibroblasts, percentage of proliferating pdpn+ cells, percentage of CD45+ cells, percentage and absolute numbers of T (CD3+) and B (CD19+) lymphocytes at day 8 p.c. in Lm (littermate controls) vehicle treated (dark grey bars), Lm DTX treated (black bars), Dm2 vehicle treated (grey light bars) and Dm2 DTX treated (red bars). Data are represented as mean ±S.D. of two independent experiments with at least three mice for each experiment. * p < 0.05; ** p < 0.01; one-way

ANOVA. **b,** Microphotograph of lymphocytic aggregates in infected salivary glands (day 8 p.c.) of lm (littermate controls) vehicle treated and dm2 vehicle treated stained for CD3 (red) and CD19 (blue). Scale bar: 100μm. qRT-PCR analysis of cxcl13 and ccl19 mRNA from Lm DTX treated (black bars, *n*=6) and Dm2 DTX treated (red bars, *n*=4) salivary glands at day 8 p.c. Represented as mean ± SD. Percentage of positive mice for ANA in Lm (littermate controls) vehicle treated (dark grey bars) and Dm2 vehicle treated (grey light bars) experimental groups at day 23 p.c. **c.** Graph summarizing the FACS data at day 15 p.c. for percentage of pdpn+, CD45+, CD3+ and CD19+ cells in Lm (littermate controls) DTX treated (black bars) and Dm2 DTX treated (red bars). Data are represented as mean ±S.D. of two independent experiments with at least three mice for each experiment. Microphotograph of lymphocytic aggregates in infected salivary glands (day 15 p.c.) of lm (littermate controls) vehicle treated, lm DTX treated, Dm2 vehicle treated and Dm2 DTX treated stained for CD3 (red) and CD19 (blue). Scale bar: 200μm.

Fig. S7. Local depletion of Pdpn+ FAP+ fibroblasts results in abrogated immune infiltration and TLS assembly.

a. Graphs summarizing the FACS data for absolute numbers of pdpn+ fibroblasts, FAP+ pdpn+ fibroblasts, absolute numbers of T (CD3+), CD4+ T cells, activated T cells (ICOS+CD44+) and B (CD19+) lymphocytes at day 15 p.c. in salivary glands of Lm (littermate controls) (black bars, *n*=6) and Dm2 (red bars, *n*=6) mice which were treated locally (L) with DTX. Data are represented as mean ± S.D. of two independent experiments with at least three mice for each experiment. * p < 0.05; ** p < 0.01; *** p < 0.001; t test. **b,** Microphotograph of lymphocytic aggregates in infected salivary glands (day 15 p.c.) of lm (littermate controls) and Dm2 mice which were treated locally (L) with DTX, stained for CD3 (red) and CD19 (blue). Scale bar: 100μm.

c. Percentage of positive mice for ANA in lm (littermate controls) L-DTX treated (black bars) and dm2 L-DTX treated (red bars) experimental groups at day 23 p.c. **d.** Graphs summarizing the FACS data for percentage of pdpn+ fibroblasts and absolute numbers of FAP+ pdpn+ fibroblasts at day 15 p.c. in mLN (distant lymph node) of Lm (littermate controls) (black bars, *n*=6) and Dm2 (red bars, *n*=6) mice which were treated locally (L) with DTX. Data are represented as mean ± S.D. of two independent experiments with at least three mice for each experiment and analysed by unpaired t test for statistical significance.

Fig. S8. Systemic and local treatment regimens for depletion of pdpn+ FAP+ cells.

Materials and Methods

Mice. *IL4rα$^{-/-}$* (1)*, IL4$^{-/-}$* (2)*, IL13$^{gfp/gfp}$* (3)*, IL22$^{-/-}$* (generated at Lexicon Genetics in collaboration with Pfizer, Boston)*, IL22rα$^{-/-}$ (*sourced from EMMA (European Mouse Mutant Archive) Sanger Center, UK)*, Rorγ$^{-/-}$* (4)*, Ltβr$^{-/-}$* (5) *and Rag2$^{-/-}$* (6) were bred in the Biomedical Service Unit (BMSU) at the University of Birmingham. Dm2 mice were provided by Prof. Doug Fearon (7). *C57bl/6* mice were from external supplier Harlan and *balb/c* mice were from an internal colony of the BMSU. All mice were maintained under specific pathogen-free conditions in the BMSU at the University of Birmingham according to Home Office and local ethics committee regulations. All mice used were 8-12 weeks old.

Salivary gland cannulation. Under ketamine/domitor anaesthesia, the submandibular glands of female C57BL/6 and knock-out mice (8-12 weeks old) were intraductally cannulated with 10^8-10^9 p.f.u. of luciferase-encoding replication-defective adenovirus (Adv5), as previously described (8). Animals were recovered from anesthesia and culled by terminal anesthesia and cardiac puncture at various time points post cannulation andsalivary glands and whole blood were harvested. Mice showing a luciferase readout with values inferior to the range for each experiment were excluded from the analysis on the basis of suboptimal virus delivery in the glands as previously described (8, 9). Systemic and local treatment regimens for depletion of pdpn+ FAP+ cells are shown in SI Appendix figure S8.

***In vivo* stimulation of salivary glands with recombinant cytokines and IL22 blockade.** 2μg/ml of recombinant IL22 (Peprotech), IL13 (Peprotech) or TNF (Peprotech) and LTβR agonist (Novus Biologicals) in PBS were directly cannulated into the submandibular glands of anaesthetized female C57BL/6 (8-12 weeks old). Glands were harvested 48 hours post-cannulation. Rat anti-mouse IL22 Ab-03 was obtained and used as previously described (10). Briefly, starting at either

day 2 or day 8 post-cannulation mice were administered a dose of 200µg of anti-IL22 antibody (Pfizer) via i.p injection followed by subsequent injections at the same dose at a frequency of three times per week. Anti-IL22 treated and untreated matched control mice were taken for analysis at indicated time-points.

Human salivary gland biopsies from patients with Sjögren's Syndrome. Minor salivary gland (mSGs) samples were obtained from Human Biomaterials Resource Centre at the University of Birmingham under ethics number 10-018. Specimens were identified among samples presenting the histological criteria for the diagnosis of SS and selected for the presence of aggregates >1 Focus score.

Histology and Immunofluorescence.

Mice

Salivary glands from virus cannulated and control mice were harvested, snap frozen in OCT over liquid nitrogen. Frozen sections of 6um in thickness were cut, left to dry overnight at room temperature. Next day they were stored in -80^0C until use. For immunofluorescence analysis, slides were allowed to reach room temperature and then fixed for 20 min in ice-cold acetone, left to dry and then were hydrated in PBS. For immunofluorescence staining, all dilutions of reagents and antibodies were made in PBS with 1% BSA. Firstly, to block endogenous biotin, sections were treated with 0.05% avidin followed by 0.005% biotin for 15 min each and washed for 5 min with PBS in between the two incubations, followed by blocking with 10% horse serum for 10 min. Slides were then incubated for 60 min with 'cocktails' containing the following primary antibodies in PBS (1% BSA); gp38/podoplanin clone 8.1.1, CD4 Alexa Fluor 647 or CD4 Pacific Blue clone RM4-5 (from BD Pharmingen), CD19 Alexa Fluor647 clone eBio1D3, CD3e biotin clone ebio500A2 (all were from eBiosciences), EpCAM APC clone G8.8 (Biolegend),

CXCL13 and CCL21 (goat polyclonal) from R&D Systems. CXCL13 and CCL21 antibodies were detected using donkey anti-goat FITC (Jackson ImmunoResearch Laboratories) then rabbit anti-FITC (Sigma-Aldrich), followed by goat anti-rabbit IgG-FITC (Jackson ImmunoResearch Laboratories, West Grove, PA). gp38/podoplanin was detected using goat anti-hamster biotin (Cambridge Bioscience, Cambridge, U.K.). Biotinylated antibodies were detected using streptavidin-Alexa Fluor 555 or 488 (Molecular Probes). Hoescht (Molecular Probes) was used for nuclear stain. All secondary antibodies were incubated for 30 min. Slides were mounted with Prolong Gold Antifade reagent (Invitrogen Life Technologies). Images were acquired on a Zeiss LSM 510 laser scanning confocal head with a Zeiss Axio Imager Z1 microscope. Digital images were recorded in four separately scanned channels with no overlap in detection of emissions from the respective fluorochromes. Confocal micrographs were stored as digital arrays of 2048×2048 pixels with 8-bit sensitivity; detectors were routinely set so that intensities in each channel spanned the 0-255 scale optimally. The LSM510 Image Examiner Software was used to process these images.

Human

Immunofluorescence (IF) Paraffin-embedded salivary glands were cut at 4µm, mounted on positively charged slides and dried at 58°C for 60 min. Immunohistochemical staining was performed on the Discovery XT Automated IHC stainer (ROCHE) and using the Ventana detection kit. Following deparaffination, washing (Ventana solution) at 75°C for 8 min, antigen retrieval was performed using Ventana proprietary Tris-based buffer solution pH8 at 95°C for 40 min. Endogen peroxidase was blocked with 3% H_2O_2 for 12 min. After rinsing, slides were incubated at 37°C for 60 min with primary antibody anti-human podoplanin (Rat, Clone NZ-1.3, ThermoFisher). Signal enhancement was performed using a linker Rabbit anti-rat HRP at 37°C

for 16 min. The HRP enzyme mediates the deposition of the tyramide fluorophore that covalently binds to the tissue at the site of the reaction (DISCOVERY Rhodamine kit). Antibodies retrieval was performed using Tris-based buffer solution pH6 at 100°C for 8 min. After rinsing, slides were incubated at 37°C for 60 minutes with primary antibody anti-human FAP (polyclonal Sheep, R&D systems), Signal enhancement was performed using a linker Rabbit anti sheep HRP at 37°C for 16 min. Tyramide fluorophore was used as previously described (DISCOVERY FAM kit). Visualization was performed with the Nanozoomer 2.0 RS (Hamamatsu) equipped with the multicolor fluorescence module and pictures analyzed with NDP.view software (Hamamatsu).

Isolation of stromal cells. Harvested salivary glands from virus cannulated or control mice were cut into small pieces and tissue digested for 40 min at 37^0C with gentle stirring in 1.5ml RPMI 1640 medium (Sigma) containing collagenase D (3.7mg/ml; from Roche), DNase I (30µg/ml; from Sigma) and 2% (v/v) fetal calf serum (FCS). The suspension was gently pipetted at 15 min intervals to break up cell aggregates. The remaining fragments were further digested for 20 min at 37 °C with medium containing collagenase dispase (3.7mg/ml; from Roche) and DNase I (30ug/ml). The suspension was then gently pipetted to break up remaining aggregates until no visible fragments remained. During the final pipetting, EDTA (Sigma) was added to a final concentration of 5 mM to further reduce cell aggregates. Cells were then passed through a 70-µm mesh, were washed twice and were re-suspended in RPMI 1640 medium containing 10% (v/v) FCS.

Isolation of leukocytes and in vitro stimulation for cytokine production. Cannulated salivary glands were harvested and chopped into small pieces and digested for 20 min at 37^0C with gentle stirring in 2 ml RPMI 1640 medium containing collagenase dispase (250µg/ml), DNase I

(25μg/ml) and 2% (v/v) FCS. The suspension was gently pipetted to break up aggregates. During the final pipetting, EDTA was added to a final concentration of 10mM to further reduce cell aggregates. Cells were then passed through a 70μm mesh with a syringe, were washed twice and re-suspended in DMEM (with 10% FCS, 1%GPS, 1% NEAA, 1%HEPES and 50μM β-mercaptoethanol) for *in vitro* stimulation culture. Isolated cells were incubated with 50ng/ml PMA (Phorbol-12-Myristate-13-Acetate), 750ng/ml Ionomycin, 10μg/ml BrefeldinA (all from Sigma) and 10μl of 10^8-10^9 p.f.u. of adenovirus for 4 h at 37°C.

Isolation of cells from human biopsies

Salivary gland biopsies were obtained and placed in 1ml of RPMI-1640 (with 2% (v/v) FCS) on ice. Once all salivary glands were collected, RPMI-1640 was removed and replaced with 2ml enzyme mix (RMPI with 2% FCS, 0.8mg/ml Dispase, 0.2mg/ml Collagenase P and 0.1mg/ml DNase I). Salivary glands were cut into small pieces and tubes were incubated at 37°C in a water bath, with magnetic stirrers. After 20 min, salivary glands fragments were very gently pipetted using a 1ml pipette, to further disrupt the tissue and release most cells. The mixture was replaced in the water bath and large fragments were allowed to settle for 30 s, after which the enzyme mix was removed. 10 ml of ice-cold FACS buffer was added (0.5% (w/v) BSA, 2 mM EDTA in PBS) and centrifuged (600^{xg} rpm, 4 min, 4°C). After centrifugation, 2ml of fresh enzyme mix was added to the digestion tube, the contents gently mixed using a 1ml pipette, and incubated, with regular gentle mixing using a 1ml pipette. After 10 min, the cells were mixed vigorously for 30 s using a 1ml pipette. Fragments were again allowed to settle, the supernatant was removed and added to the previously spun cell pellet, and 2 ml of fresh enzyme mix was added to the digestion tube. The digestion mix was then vigorously mixed using a 1ml pipette every 5 min until it was clear that all remaining salivary gland fragments

were completely digested. Supernatants were centrifuged after each removal (600^{xg}, 4 min, 4°C) until finally, each collection tube contained the entire cellular contents of the salivary gland. Cells were filtered through 70 µm nylon mesh and counted using a hemocytometer.

In vitro **stimulation of sorted stromal cells with recombinant cytokines.** Isolated stromal cells subsets were re-suspended at the same cell density in 500µl of DMEM (with 10% FCS, 1%GPS, 1% NEAA, 1%HEPES and 50µM β-mercaptoethanol) for *in vitro* cytokine stimulation assay in 48 well plates. All recombinant cytokines were reconstituted in DPBS (Sigma Aldrich). Cells were then incubated with 2µg/ml recombinant IL22 (Peprotech) alone, 2µg/ml LTβR agonist antibody (Novus Biologicals) plus 500ng/ml recombinant TNFα (Peprotech), 2µg/ml IL22 plus LTβR agonist antibody and 500ng/ml TNFα or only DPBS (Sigma Aldrich) for 24 hours at 37°C. Cells were harvested after 24 hours and taken for quantitative PCR analysis.

In vitro **stimulation of human salivary gland fibroblasts with recombinant cytokines.** Salivary gland fibroblasts were re-suspended at the same cell density in 500µl of MEM (with 10% FCS, 1%GPS and 1% NEAA) for *in vitro* cytokine stimulation assay in 24 well plates. All recombinant cytokines were reconstituted in DPBS (Sigma Aldrich). Cells were then incubated with 100ng/ml of human recombinant IL13 or IL22 (Peprotech) and/or 10ng/ml human recombinant TNFα (Peprotech) and/or recombinant LTα1β2 (R&D systems) for 48 hours at 37°C. Cells were labelled with BrDU as per manufacturer's instructions (BD Biosciences).

Flow cytometry.

Mice

Single cell suspensions were incubated with antibodies on ice for 30 min in PBS (with 0.5% BSA and 2Mm EDTA) with 'cocktails' of the following antibodies CD31 FITC clone 390, gp38 PE or

gp38 PECy7 clone 8.1.1, CD45 PERCPCY5.5 or CD45 PECy7 clone 30-F11, CD3e PE clone 145-2C11, CD3e PECY7 or BV605 clone 145-2C11, CD19 PE clone ebio1D3, CD44 FITC or PECy7 clone IM7, CD4 efluor 450 clone GK1.1 (from eBiosciences), EPCAM PECy7 or EPCAM APC clone G8.8, ICAM-1 APC, VCAM-1 PERCPCy5.5 clone 429, RANKL PE clone IK22/5, MadCAM-1 APC clone MECA-367 and ICOS AF700 clone (from Biolegend), IL22Rα APC conjugated, FAP (R&D Systems) and Ki67-Alexa 647 (BD Pharmingen). FAP was detected using donkey anti-sheep biotin (Sigma) then followed by Streptavidin APC or PE (Life Technologies).

Intracellular staining for cytokine production was performed (BD Cytofix/Cytoperm) according to the manufactures protocol. In brief, following surface staining with cocktails of desired antibodies, cells were washed in PBS (with 0.5% (w/v) BSA and 2mM EDTA), re-suspended in 150µl Cytofix/Cytoperm (BD Pharmingen) and incubated overnight at 4°C. Cells were washed twice with the BD Perm/Wash Buffer and subsequently intra-cellular IL13 PE (Biolegend) antibody was added and incubated at 4°C for 30–40 min. Intracellular staining to detect BrDU was performed as per manufacturer's instructions (BD biosciences). Afterwards cells were washed twice, re-suspended and then analyzed using a flow cytometer. Data were analyzed with FlowJo software (Tree Star). For cell sorting, stained cells were sorted using MoFlo-XDP (Beckman Coulter Inc) or FACSAria (BD). The purity of sorted stromal populations routinely exceeded 96%.

Human

Single cell suspensions were incubated with antibodies on ice for 30 minutes in PBS (with 0.5% BSA and 2mM EDTA) with 'cocktails' of the following antibodies CD45 FITC, CD31 BV605, EpCAM BV785, VCAM-1 PE, ICAM-1 APC-Fire, CD34 PEdazzle (all from Biolegend), Podoplanin

PERCPefluor710 (ebiosciences), CD11b FITC (Milteyni Biotech), CD235a FITC (Beckman Coulter).

Intracellular staining to detect BrDU was performed as per manufacturer's instructions (BD biosciences). For cell sorting, stained cells were sorted FACSAria (BD).

Single-cell PCR on human pdpn+ cells and analysis

The single-cells experiment was done accordingly to manufacturer recommendations (Fluidigm) using the C1 Single-Cell system for single-cell capture and pre-amplification. Briefly, after cell sorting, PDPN+ cells were captured with C1 medium-cell IFC (10-17uM) chip. Cells were then lysed, reverse transcribed and pre-amplified with the C1 system. Gene expression level of candidate genes was then assessed by qPCR with selected Taqman assay using the TaqMan Gene Expression Master Mix on a 96.96 Dynamic Array IFC using the Fluidigm BioMark HD system. After removal of outliers using the R package fluidigmSC (Fluidigm SINGuLAR Analysis Toolset, R package version 3.6.2) genes expression of remaining cells was calculated. The Raw Ct values were converted into expression level on a log2 scale as: log2 expression=LOD Ct-Ct, (with a value of LOD Ct of 27). Cluster analysis was completed using R v3.5.2 and RStudio v1.1.447. Complete linkage hierarchical clustering was completed using the hclust function within the stats package using Pearson's correlation as the distance measure. Samples were heuristically assigned to clusters before running principal component analysis using the prcomp function within the stats package and testing for cluster significance using the ClusterSignificance package. Genes were tested for differential expression between clusters using linear modelling within the limma package and p-values were corrected for multiple comparisons using the Benjamini-Hochberg procedure.

RNA isolation and quantitative PCR. Total RNA was isolated from salivary glands with an RNeasy

mini kit (Qiagen) and the RNA was then reverse-transcribed using the high capacity reverse transcription cDNA synthesis kit (Applied Biosystems) according to the manufacturer's specifications. Reverse transcription was carried out on Techne 312 Thermal Cycler PCR machine. Quantitative RT-PCR (Applied Biosystems) was performed on cDNA samples for vcam-1, icam-1, cxcl13, ccl19, cxcl12, ccl21, baff, il7, ltbr, IL13, IL4, il13rα, il13rα, il22 and il22rα. β-actin and PDGFRβ were used as an endogenous control. The primers and probes used were from Applied Biosystems. Quantitative real-time PCR was run in duplicates on a 384-well PCR plate (Applied Biosystems) and detected using an ABI PRISM 7900HT instrument. Results were analyzed with the Applied Biosystem's SDS software (SDS 2.3). The mean of two technical replicates (C_t values) was used to calculate the ΔC_t value for which the C_t of the β-actin was subtracted from the C_t of the target gene C_t value and the relative amount was calculated as $2^{-\Delta C_t}$. Stromal cell dependent genes on whole tissue were normalized to PDGFRβ instead of β-actin in order to account for differences in percentage of infiltrating cells between WT and knockout mice. RQ values were calculated as $2^{-\Delta\Delta C_t}$ where $\Delta\Delta Ct$ is the difference between the ΔC_t values of cannulated salivary glands and the ΔC_t of non-cannulated salivary glands. C_t values above 34 were not accepted, neither were technical replicates with more than two cycle differences between them.

Anti-nuclear antibody detection

Anti-nuclear antibody (ANA) detection was done as previously described in (9).

Statistical analysis

Statistics were performed with Prism software (GraphPad software Inc, San Diego, CA) using a student's t test and one-way ANOVA as applicable.

References

1.   Noben-Trauth N, *et al.* (1997) An interleukin 4 (IL-4)-independent pathway for CD4+ T cell IL-4 production is revealed in IL-4 receptor-deficient mice. *Proceedings of the National Academy of Sciences of the United States of America* 94(20):10838-10843.
2.   Noben-Trauth N, Kohler G, Burki K, & Ledermann B (1996) Efficient targeting of the IL-4 gene in a BALB/c embryonic stem cell line. *Transgenic Res* 5(6):487-491.
3.   McKenzie GJ, *et al.* (1998) Impaired development of Th2 cells in IL-13-deficient mice. *Immunity* 9(3):423-432.
4.   Sun Z, *et al.* (2000) Requirement for RORgamma in thymocyte survival and lymphoid organ development. *Science* 288(5475):2369-2373.
5.   Futterer A, Mink K, Luz A, Kosco-Vilbois MH, & Pfeffer K (1998) The lymphotoxin beta receptor controls organogenesis and affinity maturation in peripheral lymphoid tissues. *Immunity* 9(1):59-70.
6.   Shinkai Y, *et al.* (1992) RAG-2-deficient mice lack mature lymphocytes owing to inability to initiate V(D)J rearrangement. *Cell* 68(5):855-867.
7.   Kraman M, *et al.* (2010) Suppression of antitumor immunity by stromal cells expressing fibroblast activation protein-alpha. *Science* 330(6005):827-830.
8.   Bombardieri M, *et al.* (2012) Inducible tertiary lymphoid structures, autoimmunity, and exocrine dysfunction in a novel model of salivary gland inflammation in C57BL/6 mice. *J Immunol* 189(7):3767-3776.
9.   Barone F, *et al.* (2015) IL-22 regulates lymphoid chemokine production and assembly of tertiary lymphoid organs. *Proceedings of the National Academy of Sciences of the United States of America* 112(35):11024-11029.
10.   Ma HL, *et al.* (2008) IL-22 is required for Th17 cell-mediated pathology in a mouse model of psoriasis-like skin inflammation. *The Journal of clinical investigation* 118(2):597-607.